Glycoconj J (2015) 32:371–384
DOI 10.1007/s10719-015-9601-y

ORIGINAL ARTICLE

Impact of glycosylation on stability, structure and unfolding of soybean agglutinin (SBA): an insight from thermal perturbation molecular dynamics simulations

Swagata Halder[1] · **Avadhesha Surolia**[2] · **Chaitali Mukhopadhyay**[1]

Received: 6 April 2015 / Revised: 18 May 2015 / Accepted: 26 May 2015 / Published online: 16 June 2015

Abstract Glycosylation has been recognized as one of the most prevalent and complex post-translational modifications of proteins involving numerous enzymes and substrates. Its effect on the protein conformational transitions is not clearly understood yet. In this study, we have examined the effect of glycosylation on protein stability using molecular dynamics simulation of legume lectin soybean agglutinin (SBA). Its glycosylated moiety consists of high mannose type N-linked glycan ($Man_9GlcNAc_2$). To unveil the structural perturbations during thermal unfolding of these two forms, we have studied and compared them to the experimental results. From the perspective of dynamics, our simulations revealed that the nonglycosylated monomeric form is less stable than corresponding glycosylated form at normal and elevated temperatures. Moreover, at elevated temperature thermal destabilization is more prominent in solvent exposed loops, turns and ends of distinct β sheets. SBA maintains it folded structure due to some important saltbridges, hydrogen bonds and hydrophobic interactions within the protein. The reducing terminal GlcNAc residues interact with the protein residues VAL161, PRO182 and SER225 *via* hydrophobic and *via* hydrogen bonding with ASN 9 and ASN 75. Our simulations also revealed that single glycosylation (ASN75) has no significant effect on corresponding cis peptide angle orientation. This atomistic description might have important implications for understanding the functionality and stability of Soybean agglutinin.

Keywords Soybean agglutinin · Lectin · Glycosylation · Protein unfolding · Molecular dynamics simulations

Nomenclature

SBA	Soybean agglutinin
Gly_SBA	Glycosylated soybean agglutinin
Non Gly_SBA	Non glycosylated soybean agglutinin

Introduction

Protein glycosylation is a profusely diverse and complicated form of co- and or post-translational modifications, in which a glycosyl donor of a glycan is covalently attached to the glycosyl acceptor amino acid side chain of a protein [1]. Glycosylation is an event that modulates many physiochemical and biological properties of the protein, for instance elements of recognition during cell-cell adhesion, cell growth and differentiation, inflammation, *etc*. [2–5] . N-glycosylation occurs in more than 60 % of the proteins that possess the potential sequon "N-X-S/T" [6–8]. Most apparently, N-glycosylation has critical structural and functional roles in accelerating and decelerating protein folding, maintaining stability and integrity of the structure, increasing cooperativity, formation of secondary structure, reduction of aggregation, masking of hydrophobic surfaces and enhancing formation of disulfide bridges [7, 9–17] . However, achieving a molecular-level

Electronic supplementary material The online version of this article (doi:10.1007/s10719-015-9601-y) contains supplementary material, which is available to authorized users.

✉ Avadhesha Surolia
surolia@mbu.iisc.ernet.in; surolia@nii.res.in

✉ Chaitali Mukhopadhyay
chaitalicu@yahoo.com; cmchem@caluniv.ac.in

[1] Department of Chemistry, University of Calcutta, 92, A. P. C. Road, Kolkata 700 009, India

[2] Molecular Biophysics Unit, Indian Institute of Science, Bangalore 560 012, India

understanding of the role of N-glycan on these processes in molecular terms is still at its infancy. Studies on the affect of glycosylation on proteins can be attributed in part to an immense heterogeneity of glycans and the difficulty of obtaining them in sufficient amounts for detailed structural studies. Nevertheless, exploring the impact of glycosylation on the structural and functional aspects of protein, especially protein folding has been of considerable interest for a long time. Since glycosylation stabilizes the native conformations of many proteins against much instability especially against thermal denaturation, exploring the interplay between the addition of glycans and protein folding kinetics are of considerable contemporary interest. For example, the essentiality of glycosylation on the protein folding, stability and function is clearly emphasized from the reports of HIV 1 gp-120 protein, which needs glycosylation to reach its final folded state and the glycosylated RNase B, which exhibited higher folding rate than its nonglycosylated counterpart RNase A, though its role is limited to inducing the local conformational alterations nearby the glycosylation sequon [14, 18–20]. Studies reported here attempt to understand the role of the N-linked high mannose glycan (Man9GlcNAc2) on the glycosylated on the Soybean agglutinin.

Soybean agglutinin (SBA) is a homo-tetrameric legume lectin with a molecular weight 28,750 Da for each of its monomer. Each of its subunits is glycosylated and possesses one Ca^{++} and one Mn^{++} ions per subunit. The monomeric unit of soybean agglutinin tetramer, like any other legume lectin is composed of β sheets and adopts a tertiary structural β-sandwich fold described as the "jelly roll" motif [21]. The fold consists of two separate β-sheets of antiparallel β-strands as represented in the Fig. 1. A six stranded "back" β-sheet is positioned at the back of a curved seven-stranded "front" β-sheet and a sheet above them forms a "roof". There are several interconnecting loops in the motif to hold the sheets together. The structure is stabilized by two strong hydrophobic cores; one at the center of the three sheets and the other in the curvature of the front β-sheet. Initially, the dimer is formed by positioning the two flat six stranded "back" β sheets from each monomer in an antiparallel side-by-side fashion to generate a contiguous canonical 12-stranded β-sheet. These dimers are then oriented back-to-back to form a dimer of dimer, *i.e.,* to form a tetramer [22]. Earlier, experimental studies were performed on SBA to study the relative unfolding pathway in comparison with another tetrameric lectin, Concanavalin A (ConA) that exhibits similar tertiary structural fold sharing 45 % similarity but is unglycosylated [23]. The isothermal denaturation data has revealed that the ΔG of unfolding of SBA was much higher than that of ConA and the Tg of latter is 18 °C lesser than the former, implying higher conformational stability of SBA, which were attributed to the ionic interactions at the noncanonical subunit interface coupled with the glycosylation [23]. Previously, the monomeric subunit of SBA was also analyzed for thermodynamic parameters, subjected to size-exclusion chromatographic and dynamic light scattering studies followed by circular dichroism and fluorescence spectroscopy to assess the stability of the monomeric subunit, which showed that the monomer is well folded and the subunit interactions contribute to the overall protein stability [24] . To ascertain the remarkable stability in terms of free energy of unfolding of SBA *vis a vis* its glycosylation, the unfolding of the nonglycosylated SBA was compared with its glycosylated counterpart, which revealed that the nonglycosylated form demonstrated lower stability when compared to the glycosylated form [25] which is consistent with the isothermal and thermal denaturation profiles and which had highlighted the attributes of glycosylation for stabilization of SBA. Since, each monomer of SBA is glycosylated at ASN75 (PDB Id: 1G9F) and small units are best studied for folding dynamics, exploring SBA unfolding dynamics in the presence and absence of covalently attached glycans will complement and advance the hitherto existing knowledge on the importance of glycosylation in attaining stability. In this paper, to evaluate the thermal stability of Soybean agglutinin, SBA monomer simulations were done instead of tetramer due to two main reasons. SBA monomer serves as excellent model system for studies of multisubunit proteins (Srinivas *et al.*, 2001). Secondly, most of the studies in this field have mainly concentrated on small monomeric proteins, which have provided a lot of information about the stability and folding pathways of such proteins [24]. Thus, in concurrence with the earlier experimental evidences, our present efforts complement the findings by molecular dynamics of the monomeric SBA and further computational analysis of the relative unfolding dynamics of glycosylated (Gly_SBA) and nonglycosylated SBA (NonGly_SBA). Here, we mainly examined the influence of glycosylation on the stability and structure of SBA monomer, at 298 K and higher temperature in explicit water environment. Therefore, in the present study, we have explored the unfolding process of SBA with and without glycosylation to understand its role in structural stability and function. Our simulations not only reveal the conformations sampling of SBA, but also provides the molecular mechanisms by which glycosylation can help in folding by forming folding nucleus involving specific contacts with the oligosaccharides moiety (Sandeep *et al.*,2011).

Materials and methods

Initial structures

X-ray structure of SBA with 253 amino acids in length and 29 kDa molecular weight (PDB ID: 1G9F) was obtained from Brookhaven Protein Data Bank (http://www.rcsb.org/pdb)[26, 27]. The three-dimensional structure of SBA is known to

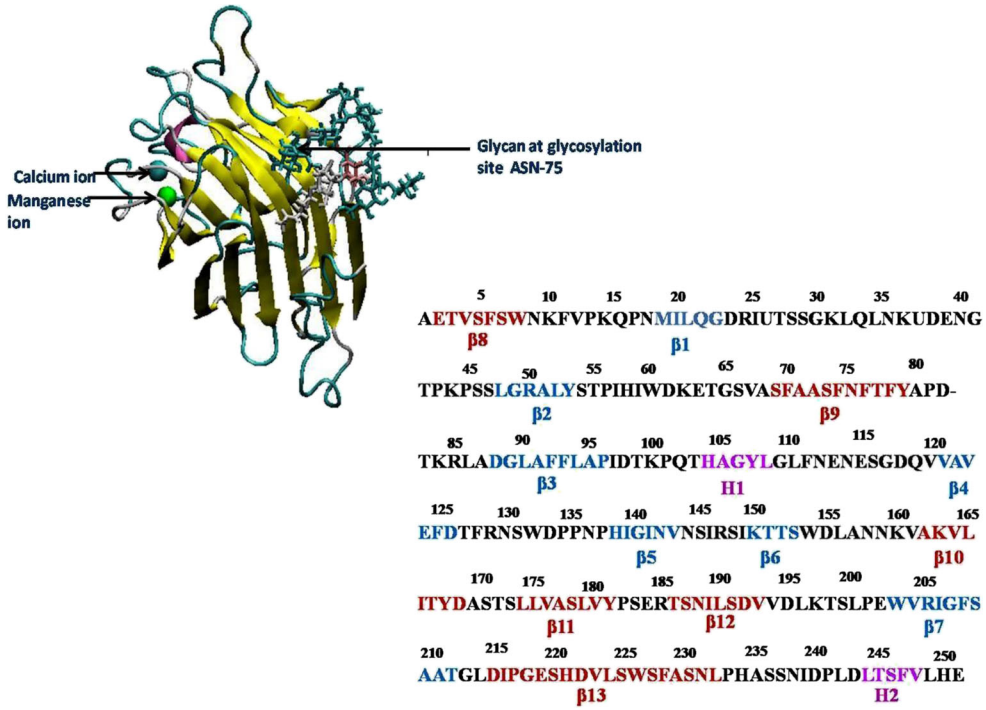

Fig. 1 Cartoon representation of three dimensional structure of SBA along with N-glycan at Asn75. The cyan and green spheres represent the Ca^{2+} and Mn^{2+} metal ions. The covalently attached oligosaccharides are shown as dynamic bonds. Amino acids sequences of SBA with secondary structure definition are shown below, where front, back beta sheets and helices are indicated by blue, red and pink colours respectively

consist of helices and anti-parallel β sheets; helices are composed of (residues104-108) and (residues244-250), respectively, the six stranded "back" β sheets composed of amino acid residues (2–8), (69–79), (162–169), (174–181), (186–193) and (220–232), whereas the seven β strands of "front" β-sheets are constituted by amino acid residues (18–22), (48–53), (88–96), (121–126), (138–143), (150–153) and (203–212) (Fig. 1) [27] . The existing glycan ($GlcNAc_2$) was replaced at Asn-75 with high mannose glycan ($Man_9GlcNAc_2$) obtained from SWEET II database [28]. The molecular models for each glycosylated and nonglycosylated SBA was built with the general molecular modeling program, CHARMM [29].

Molecular dynamics simulations

Molecular mechanics and dynamics simulations were performed on IBM Blade Server using NAMD-2.7 package for all variants [30]. We have performed normal and thermal MD simulations for both the glycosylated and nonglycosylated monomers of SBA in explicit solvent systems to assess their inherent flexibilities. The monomeric systems (with and without N-linked glycans) were prepared in CHARMM using all atom CHARMM 31b1 force field and modified TIP3P water model [31] . TIP3P, three-site rigid water model was used to solvate Gly_SBA and NonGly_SBA systems. Care was taken to remove water molecules, if they were closer than 2.6 Å to any heavy atoms of the proteins. In summary, each system containing protein and water molecules were simulated under periodic boundary conditions with an orthogonal box of defined dimensions.

MD parameters

Subsequent to system preparation, the structure was minimized by 10,000 steps, to remove the steric clashes. After minimization the systems were gently heated from 0 K to 298 K and then maintained in isothermal-isobaric ensemble (NPT) with a target temperature of 298 K and at constant pressure of 1 bar. The Langevin dynamics was employed to maintain temperature at 298 K and Nośe-Hoover-pistons were applied for pressure control 1 atm [32]. The long range interactions were computed employing particle mesh Ewald method [33] and the short range interactions were cut off at 10 Å. The volume of the box was equilibrated for 350 ps at constant temperature and pressure. Following equilibration, the systems (glycosylated and nonglycosylated) were subjected to production dynamics and this phase continued for 100 ns with a time step of 2 fs maintained in isothermal and isobaric ensemble (NPT). SHAKE algorithm is used on all hydrogen-heavy atom bonds to permit a dynamics time step of 2 fs [34]. Elevated temperature MD simulations were performed for both the SBA systems (Gly_SBA and NonGly_SBA) to unfold the protein at 380 K with identical parameters, as discussed above. Each of the simulations of glycosylated and nonglycosylated SBA at two temperatures were repeated

two times using different random number seeds for assigning different starting velocities. The simulations have been called S1 and S2 respectively. We used VMD for molecular visualization and CHARMM is used to analyse the four systems [29, 35].

Trajectory analysis

The production simulations have resulted into trajectories, which were subjected to standard analyses including root-mean square deviation (RMSD) relative to the initial structure and root-mean-squared fluctuations (RMSF) relative to the average positions. In addition, few more analyses were carried out to better compare the Gly_SBA and NonGly_SBA simulations. These include calculations of solvent accessible surface area (SASA), native contacts and number of hydrogen bonds in protein and cis peptide angle distributions. Contact maps were done to account the changes in secondary structures and stability of monomeric SBA structures were analyzed by identifying the stable salt bridges and interaction of protein residues with oligosaccharides.

Results and discussions

Glycosylation has a repertoire of functionalities and rendering structural stability to the protein can be perceived as one of its major attributes. In this arena, our present effort focuses on the criticality of glycosylation of N-linked glycan ($Man_9GlcNAc_2$) in upholding the structural stability of a monomeric unit of soybean agglutinin through complex molecular dynamics simulations. For this, glycosylated and non-glycosylated SBA were generated from the 3D coordinates of SBA (PDB ID: 1G9F). The covalently attached $GlcNAc_2$ was removed and replaced with the high mannose glycan - $Man_9GlcNAc_2$, which was then used in this study (see Fig. 1). MD simulations provide promising atomic-level description of protein stability when subjected to various physiological conditions, like temperature in the presence and absence of covalently attached glycan to recount the impact of glycosylation in maintaining the structural integrity of the variants of SBA. A spectrum of analyses was performed to shed light on the relative structural stability of Gly_SBA and NonGly_SBA.

Initial conformation of the oligosaccharide moiety

We have analyzed the conformational changes occurring in the oligosaccharide moiety of glycosylated SBA during the first 10 ns of simulations. The flexibility of the oligosaccharide has already been investigated in earlier studies using MD simulations [36, 37]. Molecular dynamics simulation of oligosaccharides and their conformation in the crystal structure of lectin-carbohydrate complex was reported by Qasba *et al.* [38]. However, in those studies the majority of the SBA protein was restrained and the simulations were for short durations. Since our current study involved multiple numbers of long simulations without any restraints, it might give a more realistic picture of the conformational dynamics of the oligosaccharide moiety. Table 1 lists the average values of the various dihedral angles of linkages in the oligosaccharide along with the standard deviations over the initial 10 ns simulations for each of the two trajectories for glycosylated SBA at 298 K. For the purpose of comparison we have listed in Table 1, the average and standard deviation values of the corresponding dihedral angles. These dihedral values have been reported from crystral data by Petrescu *et al.* [39]. In glycosylated SBA, oligosaccharide contains 11 sugar residues (254–264) [Supporting Figure S5], the structure of the which was investigated by high resolution 1H NMR spectroscopy [40]. The values that have been obtained from this present work [Table 1] are similar to the MD and NMR data obtained by Homans *et al.* and Olsen *et al.*[41]. For example, the average values for ϕ1 for $GlcNAc^{254}$β (1–4) GlcNAc255 linkage in our simulations ranged between −73 and −86° and ψ1 was ranged between 154 and 160°, which were close agreement with values reported by Homans *et al.* Table 2 contains the glycosidic dihedral angles (γ) measured as Cγ -N-C1-O5 (between Cγ-N of ASN-75 and C1-O5 of GlcNAc) and the chi (χ) angle measured as N-Cα-Cβ-Cγ for the side chain of Asn-75. For nonglycosylated SBA the average value of the χ dihedral angle of the Asn-75 side chain was found to vary between −52 and −73 ° in two different simulations and the standard deviations were as high as 23°. However in glycosylated SBA average value of χ ranged between −44 and −48° with a maximum standard deviation only 6°. It is seen that glycosylation has restricted the rotation of the Asn-75 side chain to a relatively smaller range. These results are consistent with the previous results of ECorL, where due to glycosylation at ASN-17, restriction of rotation was observed [42].

Dynamics of glycosylated and nonglycosylated SBA systems at different temperatures

Difference in stability of monomeric forms of Gly_SBA and NonGly_SBA

The relative stability of the two SBA systems was illustrated by the root-mean-square deviations (RMSD) from the corresponding initial structures as a function of time. The four individual MD simulations for Gly_SBA and NonGly_SBA were performed for 100 ns at 298 K and 380 K. It was observed that the systems were fluctuating at elevated temperature than at the normal temperature. The backbone coordinates of Gly_SBA and NonGly_SBA were regarded as initial starting structures for calculating the RMSD. Cα RMSD plot (Fig. 2a,c) shows the displacement from the initial starting

Table 1 ϕ and ψ Angles (in degrees) of the individual disaccharides from the Glycosylated Soybean **a**gglutinin (SBA)

	$\phi=O_5\text{-}C_1\text{-}O_X\text{-}C_X$		$\Psi=C_1\text{-}O_X\text{-}C_X\text{-}C_{X\text{-}1}$	
	S1	S2	S1	S2
$GlcNAc^{255}$ -β(1–4)-$GlcNAc^{254}$	−86±3	−73±3	160±5	154±5
$GlcNAc^{256}$ - β (1–4)- Man^{255}	−38±4	−42±3	−44±4	−48±4
Man^{257}- α(1–6)-Man^{256}	45±4	48±4	−142±2	−148±4
Man^{258} -α(1–3)-Man^{257}	−10±5	−16±4	−150±10	−142±8
Man^{259} -α(1–2)-Man^{258}	−8±2	−13±2	−155±8	−167±7
Man^{262} -α(1–3)-Man^{256}	−134±4	−139±4	−162±3	−168±3
Man^{261}- α(1–2)-Man^{260}	13±2	19±2	162±2	−164±4
Man^{260}- α(1–6)- Man^{257}	−5±3	−9±4	−153±7	−144±6
Man^{263} - α(1–2)-Man^{262}	−112±5	−118±6	−158±3	−150±3
Man^{264}- α(1–2)-Man^{263}	−12±6	−18±6	−168±8	160±8

structures of each Gly_SBA and NonGly_SBA monomeric forms at 298 K for S1 and S2 simulations, respectively. It was noted that RMSD of Gly_SBA (Fig. 2a) was close to 2.2 Å at 40 ns in S1 simulation and remains almost same during entire simulation time (2.2±0.2 Å); however the NonGly_SBA initially attained a value of 2.0 Å but after 40 ns it became 2.7 Å and finally attined 3.2 Å indicating that at room temperature, the NonGly_SBA (2.6±0.4 Å) was marginally more flexible compared to the Gly_SBA monomer. In case of S2 simulation (Fig. 2c), for glycosylated monomer RMSD attained 2.7 Å (2.3±0.2 Å and for nonglycosylated monomer RMSD reached 3.3 Å (2.8±0.4 Å) at the end of the simulation. Likewise, RMSDs of individual two simulations were compared at higher unfolding temperature of 380 K (Fig. 2b, d). As seen from (Fig. 2b) the initial RMSD of Gly_SBA was 2.0 Å and stabilized at 6 Å after 40 ns till 100 ns (5.1±1.4 Å), while the NonGly_SBA had an initial RMSD greater than 3 Å and gradually attained ~4 Å within 30 ns and reached 7.5 Å at 100 ns (5.6±1.3 Å).In case of S2 simulation at 380 K (Fig. 3b), RMSD of the glycosylated monomer reached 6 Å (5.2±1.1 Å) and nonglycosylated monomer reached 7.5 Å (5.8±1.3). Thus the simulations at higher temperature clearly reflect that the structural deviation become more prominent in NonGly_SBA, as the non-glycosylated monomeric form starts to unfold more quickly than the glycosylated form at two different simulations.

To assess the flexibility of individual residues we have also performed residue-wise RMSD analysis of all simulations at both the temperatures. It was observed that at 298 K from two individual simulations, the RMSD of Gly_SBA and NonGly_SBA residues remained in the range of 2 Å and 2.5 Å, respectively (Fig. 3a, c). It was also seen that for both the monomers the C-terminal residues are more flexible due to high protein–sugar interaction. It was interesting to note that from two simulations at 380 K the RMSD of the residues of non-glycosylated SBA monomer showed considerable increase at elevated temperature (Fig. 3b, d), during the entire 100 ns of trajectory, while the fluctuations in the glycosylated form of SBA were restricted to the C-terminal only. This indicates that there is difference in the dynamics of the individual residues in the two forms of the monomer. Flexibility of the individual sugar residues from their initial position can be understood from backbone RMSD (Figure: S1). On examining the distribution of the dihedral angle of the glycosidic bonds with the entire simulation time (Figure: S1 (c) – (l)), we can predict that the terminal GlcNAcβ1-4 linkage is rigid compared with the other linkages due to a high prosperity of the interaction with the protein.

Table 2 Glycosidic Dihedral Angle (γ) and Chi (χ) Angle for Asn75 of SBA.B..oth angle values are expressed in degrees

	NonGly_SBA		Gly_SBA	
	S1	S2	S1	S2
γ (Cγ -N-C1-O5)			54±8	62±10
χ (N-Cα-Cβ-Cγ)	−73±18	−52±23	−48±5	−44±6

The glycosidic dihedral angle (γ) measured as Cγ -N-C1-O5 (between Cγ-N of Asn-75 and C1-O5 of GlcNAc) and the chi (χ) angle measured as N-Cα-Cβ-Cγ for the side chain of Asn-75. The columns S1 and S2 correspond to dihedral angles obtained from the two independent simulations carried out with different initial velocity

Solvent accessible surface area

Protein–solvent interactions are crucial to protein stability and biological activity and as such are important in protein folding and unfolding. The contribution of protein–solvent interactions to thermodynamic parameters of protein unfolding has been studied extensively. One approach is based on connecting thermodynamic measurements with the change in protein solvent-accessible surface area on going from the

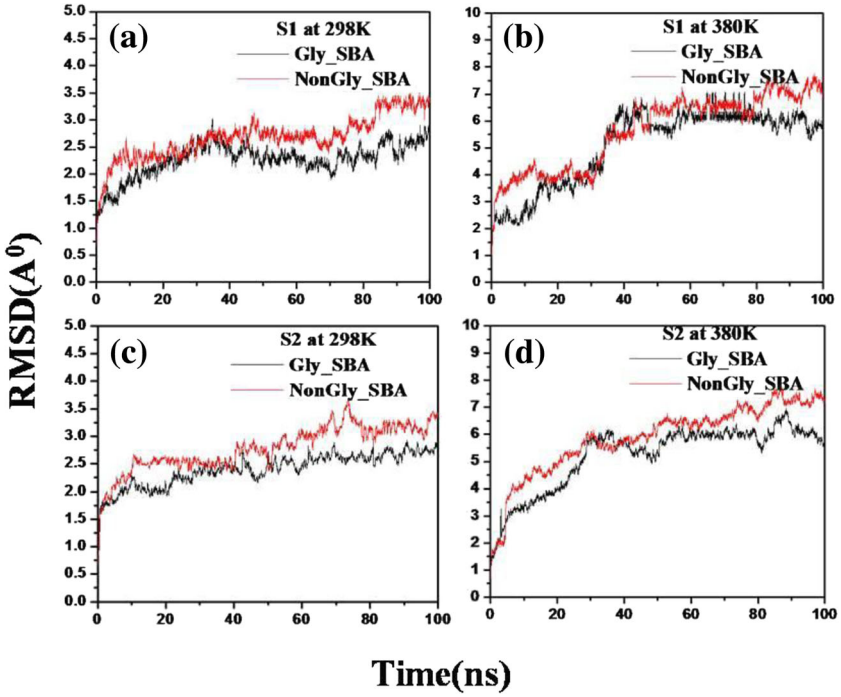

Fig. 2 Root mean square deviations (RMSDs) from initial structure for the both protein backbone as a function of time (**a**) for S1 simulations at 298 K (**b**) for S1 simulation at 380 K (**c**) for S2 simulations at 298 K (**d**) for S2 simulation at 380 K, respectively

native to the unfolded state. The solvent-accessible surface area (SASA) is used often to monitor the unfolding process. The solvent exposure of both hydrophobic and hydrophilic amino acid residues continuously are increased during the unfolding simulations at 380 K. When we plot SASA on averaging the data obtained from individual two simulations as a function of time at 298 K and 380 K for both systems (Fig. 4a, b), it is evident that SASA for glycosylated and nonglycosylated monomers remain in the range of 11700 $Å^2$ (11715±286 $Å^2$) and 12500 $Å^2$ (12589±296 $Å^2$), respectively

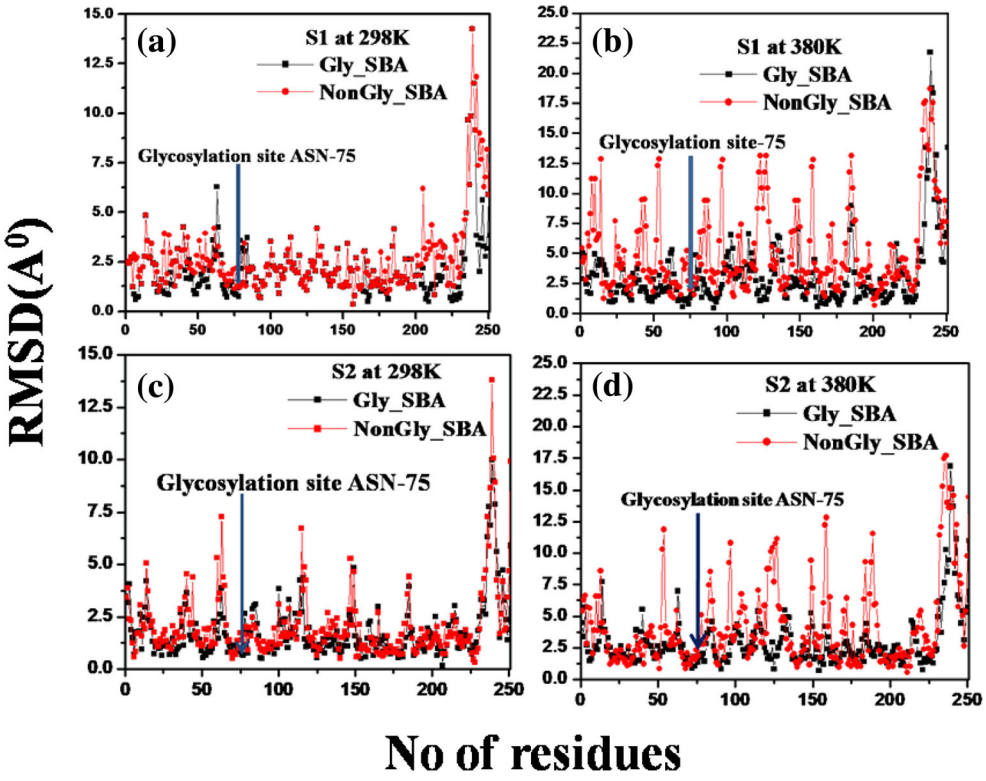

Fig. 3 Residue wise RMSD for both monomers (**a**) for S1 simulations at 298 K (**b**) for S1 simulations at 380 K (**c**) for S2 simulations at 298 K (**d**) for S2 simulation at 380 K respectively

at 298 K. With increase of temperature considerable fluctuation of solvent accessible area is observed for both monomers. For Gly_SBA SASA sharply increases from 11000 $Å^2$ to 14000 $Å^2$, whereas SASA for Non Gly_SBA becomes 15000 $Å^2$ from 11000 $Å^2$ within first 20 ns of the simulation time and attained a value of 15000 $Å^2$,16000 $Å^2$ respectively at the end of the simulations. This might indicate that the hydrophobic core remains more intact in case of Gly_SBA and these explain the previous experimental observation of higher thermodynamic stability for Gly_SBA compared to NonGly_SBA at higher temperature. To account for the contribution of hydrophobic residues in the change of SASA at higher temperature, we have calculated SASA for hydrophobic residues (Figure:S2) for both systems separately. These plots show that average SASA value of hydrophobic residues increases from ~9000 $Å^2$ to ~11000 $Å^2$ for Gly_SBA and ~9000 $Å^2$ to ~12000 $Å^2$ for NonGly_SBA. This clearly indicates loss of hydrophobic contacts being crucial for unfolding.

Loss of native contacts for the Gly_SBA and NonGly_SBA at unfolding temperature

Loss of native contacts is one of primary events associated with unfolding of protein . The protein unfolding process generally involves the transition of the protein backbone from an ordered to a disordered state. Thus, hydrogen bonds and native contacts in proteins are destroyed as this process proceeds. Therefore, we calculated the reduction in number of contacts as a function of time in both temperatures for both monomeric systems. We have calculated the protein-protein backbone contact defined as any two Cα atoms which are within 4 Å. If we compare the number of contacts within protein residues of both monomers (initial first 10 ns and final 10 ns) on averaging the data of individual two simulations at 298 K and 380 K, (Figure S3) it was observed that at 298 K initial 10 ns number of contacts between protein-protein backbone for Gly_SBA (39099±401) is higher than the NonGly_SBA (38569±445) but last 10 ns it becomes 38089 ±455 and 37000±453 respectively. In case of both monomers at 380 K, the number of contacts initially was 35000±450 and 34000±452, finally contact value becomes more reduced in NonGly_SBA (27500±470) than Gly_SBA (29000±468) indicating unfolding. These results not only supports the aforesaid RMSD and SASA values but are also consistent with the previous experimental results observed by Sinha and co workers (25) . Therefore melting process is accelerated across the chain for the Nongly_SBA as the loss of contacts is significantly more than the Gly_SBA

Number of hydrogen bonds rapidly decreases in NonGly_SBA at unfolding temperature

To make the analysis more stringent, the protein-protein hydrogen bonds for both the monomers were analyzed with time. We have calculated the number of backbone-backbone H-bonds where H-bond is defined when the distance between O of C=O and H of NH groups is within 2.4 Å and the hydrogen bond angle [defined as the angle between C=O…H] is within 120^0. From the plot (Figure S4), it is observed that the average number of intra-molecular hydrogen bonds for Gly_SBA (332.97±37.60) and NonGly_SBA (300.31± 34.98) does not vary asignificantly at 298 K. At 380 K, (Fig. 5) both monomers show a greater number of hydrogen bonds loss due to unfolding. Hydrogen bonds are mainly lost in loop regions between ASP133:O- ARG129:HE, MET18:HN-GLN15:O, SER213:HN- SER46:O for Gly_SBA and SER171:HG1-ILE59:C, MET18:HN-GLN15:O and ASP169:OD2-LEU174:H for nonglycosylated monomer respectively. Effect is more prominent for non-glycosylated form. This supports the higher stability of Gly_SBA demonstrating that structurally important and persistent hydrogen bonds in glycosylated monomer are consistently less influenced by the thermal perturbation. Moreover, the oligosaccharide moiety (Figure S5) showed a dynamically stable interaction mainly with the residues SER29, VAL161, PRO182 and LEU224 all of which are distantly positioned from the site of glycosylation, ASN75 in the amino acid sequence (Figure S6). One important thing is that the N-linked

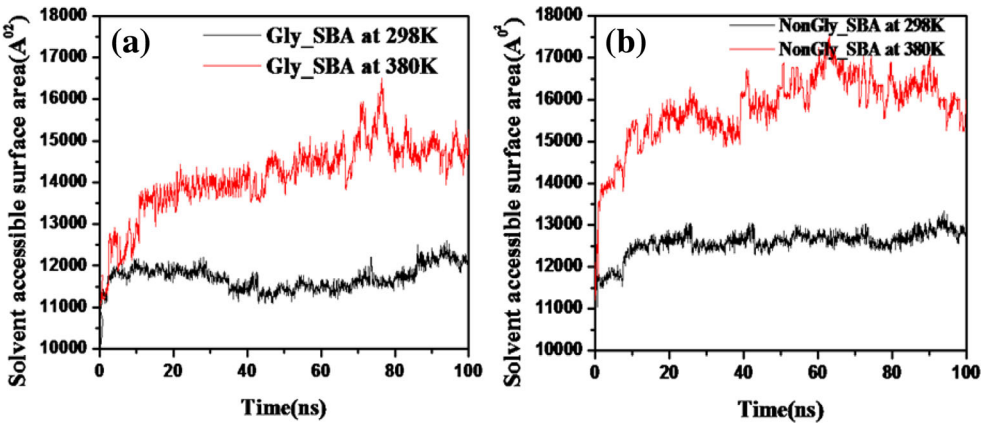

Fig. 4 Solvent accessible surface area of the whole protein (**a**) glycosylated monomer with time at298K and 380 K (**b**) nonglycosylated monomer with time at 298 K and 380 K

GlcNAc residue interacts with the protein *via* hydrophobic and hydrogen bonding with ASN 75. The interactions between VAL161, PRO182, SER225 and oligosaccharides are hydrophobic in nature. Types of interactions between protein and sugar in SBA are discussed in detail below. Therefore, it is possible that glycosylation helps in forming long-range contacts between amino acids, which are separated in sequence and thus provides a stable core.

Interaction of amino acid residues with oligosaccharides

One factor that probably accounts for the greater stability of SBA over the other legume lectins is the presence of an N-linked glycan in SBA [43]. SBA has three potential glycosylation sites out of which only one, ASN 75 is glycosylated due to the perfect geometry of this site. It has been reported that glycosylation affects both the structural elements and the global stability of proteins. The N-linked glycans are large hydrophilic structures. The volume of 11 residue carbohydrate attachment is 1800 $A^{\circ 3,}$ This size is therefore significant in comparison to the monomeric protein size, which is 30,000 A° [3](25). A total of 27 hydrogen-bonding interactions and 53 hydrophobic interactions between glycan and amino acid residues were reported by Sinha *et al.* (27), but out of the 27 hydrogen bonding, only two interactions are found to be intra subunit whereas the rest are inter-subunit interactions. Similarly, only 13 out of 53 hydrophobic interactions are intra-subunit in nature (27). In the previous study, they showed that role of the two proximal GlcNAc residues in tethering the glycans attached to one subunit to the side chains of amino acid residues of an adjacent subunit at the noncanonical interface but in our present study we are able to show further that the two proximal GlcNAc mainly interacts hydrophobically with the amino acid residues such as VAL161, PRO182, SER225. Two important hydrogen bonding interactions are found between ASN75 with GlcNAc254 through ASN9 (Fig. 6a) Details of interactions are given in the Table 3. As protein-sugar interactions are crucial for many biological processes. We have calculated the interaction energies of oligosaccharides with individual surrounding amino acid residues and partitioned the total interaction energy into electrostatic and van der Waals (vdW) contributions (Fig. 6b). The plot shows that the main stabilization has originated from van der Waal interaction between sugars and the proteins as the oligomannose glycan is well embedded in the clefts and cavities on the protein surface. Electrostatic interactions (−7.56 kcal/mol,-31.89 kcal/mol) are observed between ASN 9, ASN 75 and terminal sugars due to hydrogen

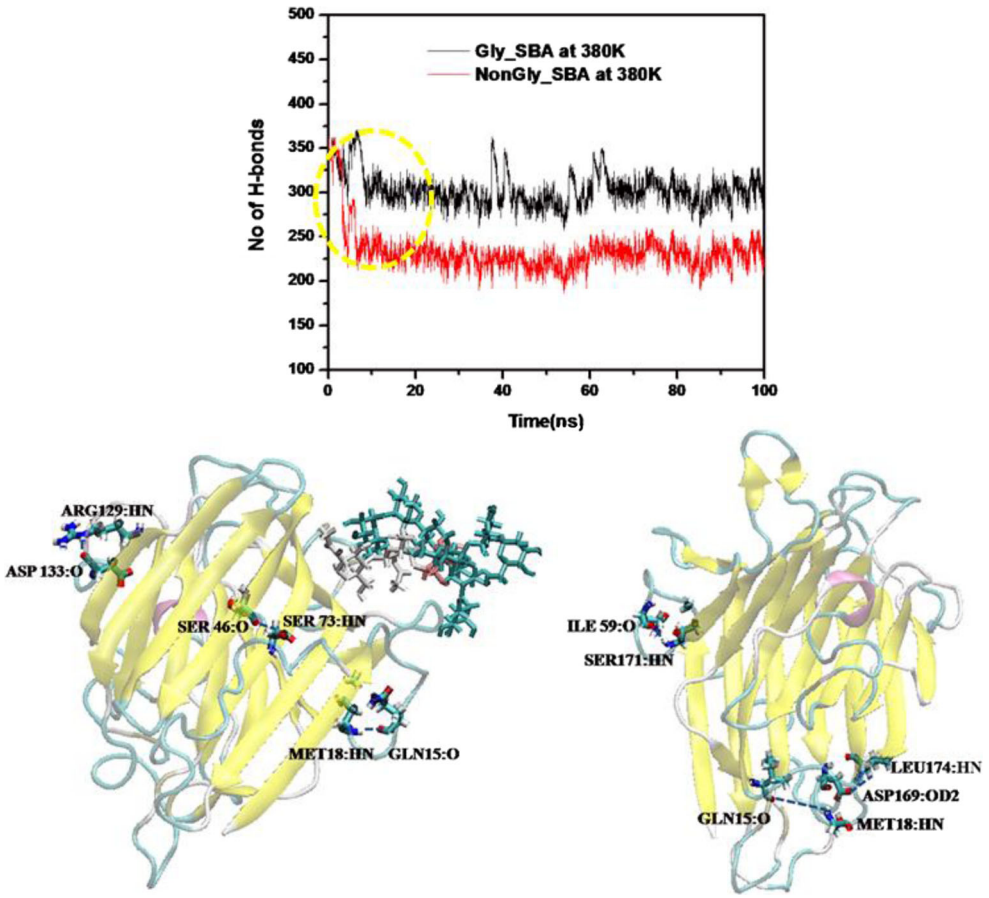

Fig. 5 Number of H bonds within protein-protein backbone with time for glycosylated, and nonglycosylated monomer at 380 K. Hydrogen bonds in the loop regions for glycosylated, and nonglycosylated monomer at 380 K are shown below as dynamic bonds

bonding. Van der Waals interactions are observed in between VAL161, PRO182, SER225 and terminal *N*-acetylglucosamine.

Effect of glycosylation on cis peptide angle distribution for both monomers at unfolding temperature

Glycosylation site of SBA is ASN 75 residue, which is located on a beta strand ("back" beta sheet) that is connected to a cis-peptide bond through a loop. The cis-peptide bond is between residues ALA87 and ASP88. Both of these residues are important for carbohydrate binding by SBA. The cis-peptide also stabilizes the calcium binding site, which is important for substrate binding [44]. Hence, glycosylation may partly influence these cis-peptide forming regions. While the variation of cis-peptide angle (ω) was negligible at 298 K, at 380 K the variations of ω over time for both glycosylated and nonglycosylated systems (Fig. 7a, c). Corresponding cis-peptide angles (ω) ranged between −25° to 25° and −30° to 30° for both systems, respectively, indicating that single-site glycosylation has no significant effect on its orientation up to 100 ns simulation. On comparing the cis peptide angle distribution plot (Fig. 7b, d), we clearly observed the difference between the two peaks. Glycosylated peak was sharper than the other due to more protein-sugar interactions.

Effect of temperature on the functionally important residues

Several Amino acid residues namely, ALA 87, ASP 88, ALA 105, PHE 128, ASN 130, LEU 214, ASP 215 and ILE 216 are involved in carbohydrate binding by SBA. Some of the residues form H bonds with other amino acids (ASP88: OD-PHE128: HN, ALA105:NH-ASP133:OD, ASN130:HN-ASP133:OD2, LEU214:O-ARG85:NH, ASP215:O-ARG85:NH). The root mean square fluctuation (RMSF) is defined as the fluctuation of atoms from their mean position and is a good measure of the dynamic flexibilities of the residues. It is noticeable that RMSF values for ALA87, PHE 128, LEU 214, ASP 215 and ILE 216 show a relative increase in NonGly_SBA than in its Gly_SBA counterpart at both the temperatures, further indicating that SBA deprived of glycosylation has an impact on these residues of carbohydrate binding region (Table S1). However, at 380 K there is marked difference in fluctuations between the glycosylated and nonglycosylated forms for these residues. ASP88, ALA105, ASN130 show relatively small fluctuations 1.21±0.04 Å, 2.58±0.02 Å, 1.90±0.05 Å in glycosylated form and large fluctuation 2.07±0.04 Å, 4.54±0.02 Å, 2.82±0.05 Å in nonglycosylated form respectively. ALA105, being in the loop region shows highest fluctuation (4.54±0.02 Å) in nonglycosylated_SBA monomer than the other residues at 380 K. In metal binding region GLU124, ASP126, ASP133 and HIS138 are involved (Figure S7). GLU124 and ASP133 show more RMSF fluctuation in Gly_SBA monomer and ASP133 shows highest fluctuation in nonglycosylated form at 380 K. ASP 126 shows least fluctuation in both forms at 380 K, indicating higher stability towards the metal binding.

Probability of forming H-bond decreases more in case of loop regions for both monomeric systems at 380 K

The persistence of H-bonds are identified as a key descriptor of structural response to environment and hydrogen-bond loss in distinct loop regions and ends of critical β sheets suggest

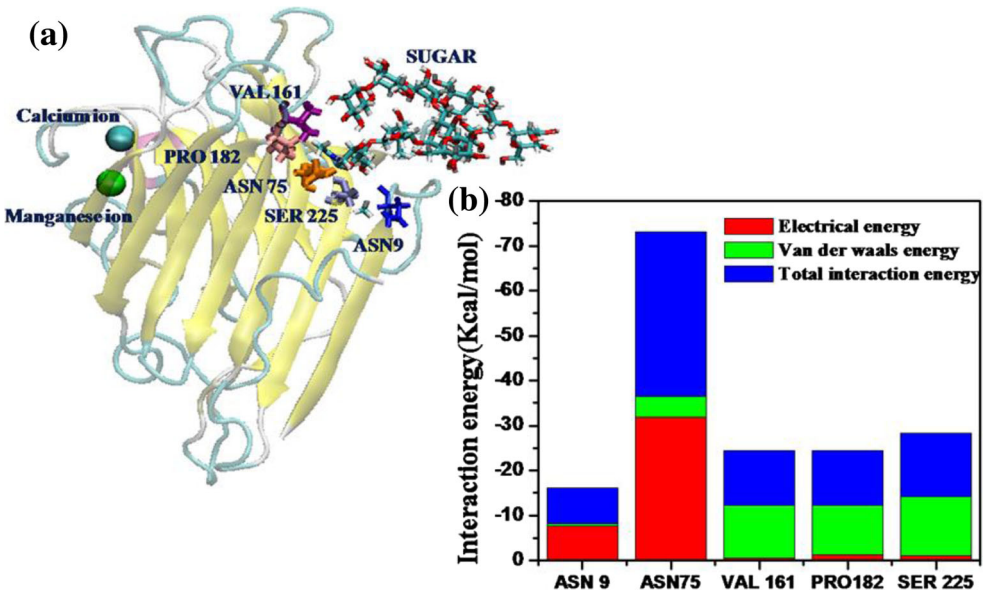

Fig. 6 (**a**) Pictorial representation of interacting amino acid residues (ASN 9, ASN 75, VAL161, PRO182 and SER225) with carbohydrate present in glycosylated SBA (**b**) Interaction energy between protein residues with carbohydrate present in glycosylated SBA

Table 3 Some important intra-subunit glycans-protein interaction in Glycosylated SBA

Sugar residue	Protein residue	Distance (Å)	Type of Interaction
N-Acetylglucosamine254	ASN9	2.3	Hydrogen bonding
	ASN75	2.5	Hydrogen bonding
	VAL161	3.9	Hydrophobic
	PRO182	2.7	Hydrophobic
	SER225	2.3	Hydrophobic
N-Acetylglucosamine255	ASN9	4.9	Hydrophobic
	ASN9	3.6	Hydrophobic
	ASN9	3.4	Hydrophobic
	ASN9	3.4	Hydrophobic
	ASN9	3.4	Hydrophobic
	ASN9	2.4	Hydrophobic

initial regions of unfolding. From the unfolding trajectories, if we see the snapshots for both the monomers we can see that residues, which are forming the loop regions (31–54,102–174) unfold relatively quicker than the other residues which constitute the stable β sheet and α helix. For glycosylated monomer H-bonds occur mainly in the loop region between the backbone atoms of ALA1:NH-ASP61:OD2, ASP133:O-ARG129:HN, TRP154:NH-PRO137:O,MET18:HN-GLN15:O, SER213:HN- SER46:O, to identify these dynamically less stable or low occupancy H-bond in loop region, we calculate H-bond distance probability over the whole simulation time. From the (Fig. 8a) we predict that the H-bond between ALA1 and ASP 61 is retained almost throughout the simulation time where as others show a tendency to break. In case of nonglycosylated monomer (Fig. 8b), H-bonds occurs mainly in the loop region between the backbone atoms of SER171:HN-ILE59:O, MET18:HN-GLN15:O, ASP169:OD2-LEU174:HN, but from the H-bond distance probability plot we can see that, at unfolding temperature probability of forming of H-bond in loop regions becomes lesser as the H-bond distance increases.

Changes in secondary structure during the unfolding process at 380 K by contact map

The contact region is largely made up with hydrophobic and polar residues, although few crucial aromatic, acidic and basic residues are involved. The C_α atoms of ith and jth residues are in contact if they are within 7.0 Å. The structures have been averaged over 10 ns time frames from different time points (initial, middle and final) and plotted in Figs. 9 and 10. The distance of each native contact during the simulations is

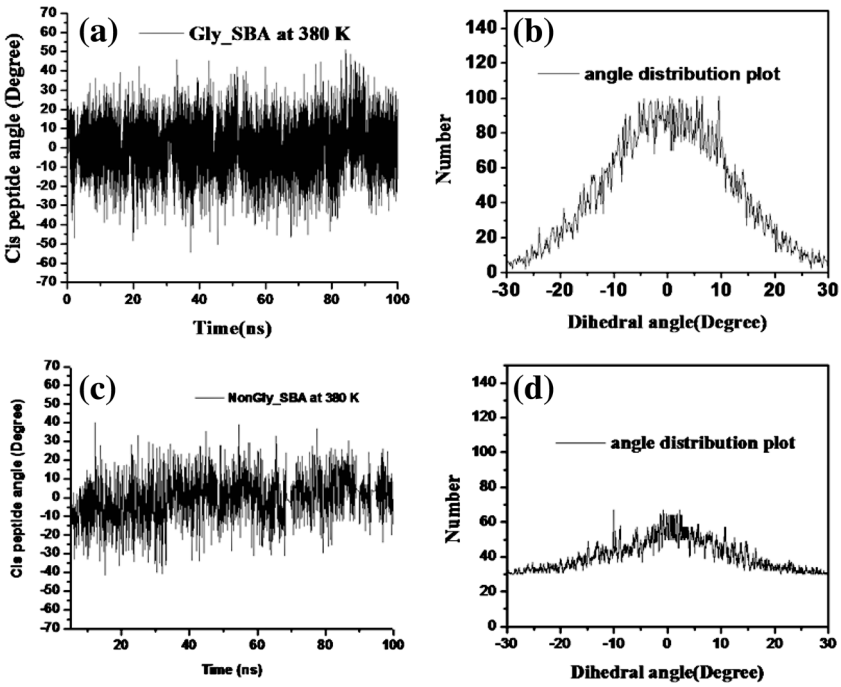

Fig. 7 Cis peptide angle variation with time (**a**) for glycosylated monomer at 380 K (**c**) for nonglycosylated monomer at 380 K. Angle distribution plot (**b**) for glycosylated monomer at 380 K (**d**) for nonglycosylated monomer at 380 K

depicted in magenta, blue, sky, light green, green, yellow, orange and red in increasing order. Contact map clearly shows that front β4 strand is in close contact with front β5 strand and back β5 strand with β6 strand. Time evolution contact map shows loss of contact between the loop region connecting front β4 and β5, same loss of contact is also found in loop regions of back β5 strand with β6 strand. Loss of contact is more prominent at last 10 ns time averaged contact map in nonglycosylated monomer than glycosylated monomer at 380 K where as contact between β1, β2 strand β2, β3 are also altered at the end of the simulation.

Changes in secondary structure during the unfolding process at 380 K by secondary structure analysis

The three-dimensional structure of native SBA is known to consist of helices and anti parallel β sheets, as discussed earlier. The single site of glycosylation (Asn 75) resides in the loop connecting two β sheets (48–53 and 88–96). When we consider the change of secondary structure of protein as a function of time during the unfolding process at 380 K for both monomers the relative ease of unfolding of the secondary structural elements of the two monomers becomes apparent. Here secondary structures of both monomers at unfolding temperature are analyzed by VMD software (version 1.5) and Ramachandran plot. Secondary structures in VMD timeline are analyzed at 50 ns time interval of both monomers. It is interesting to see the secondary structure (Figures S8, S9), in case of glycosylated monomer, that residues nearest to the glycosylation site remain in the beta sheet configuration throughout the simulation time, indicating glycosylation reduces the structural flexibility of the neighboring residues during the unfolding MD. Ramachandran plots (Figure S10, S11) are done from time averaging structure (initial, middle and final 10 ns). Backbone phi, psi values are calculated from the time averaged structures. On comparision of backbone dihedrals, we can see that initially both monomers consist of β sheets (ϕ=−110° to −140°,ψ=110° to 140°) and α helices (ϕ=−57°,ψ=−47°), but with time, β sheets and α helices have been destroyed. Last 10 ns average structure indicates the low interactions between closely folded parallel segments (β sheets) and helical segments.

Effect of salt bridges

Salt bridges have been proposed to play a crucial role in promoting thermostability in proteins, yet they appear to make little contribution to protein stability at room temperature. Two charged residues are completely compensated by favourable interactions within the salt bridge and with the rest of the protein. Therefore to further strengthen our finding on the enhanced unfolding dynamics of NonGly_SBA over Gly_SBA, the stability of solvent-exposed salt-bridges which may stabilize some thermophilic proteins, in particular between domains and secondary structure elements were examined [45]. Salt-bridges are likely to be more stabilizing at high temperatures, as the desolvation cost for fixing an ion pair decreases with the temperature [46]. For this study, some salt bridges in glycosylated monomer such as ASP23 - LYS44, ASP215 - ARG85, GLU39 - LYS36, ASP192 - LYS150, ASP118 - LYS100, ASP195 - LYS197 were found to be conserved all through the simulation time, (Table 4). These long-lived interactions bridge distant parts of the proteins and may thus be identified as affecting structural integrity. Some salt bridges are present for more than 50 % of the simulation time and some salt bridges are formed and destroyed such as ASP98 - LYS100, ASP82 - ASP84, GLU113 - ARG147. The most notable among these interactions is ASP222-LYS31, which is broken in the unfolding simulation at 380 K. It is located at the N terminus region and may be important for initial unfolding of glycosylated monomer. Nonglycosylated monomer on the other hand, showed only GLU39 - LYS36, ASP192 - LYS150, ASP23 – LYS44 are preserved throughout the simulations, see (Table 5). The findings of this study provide a complementary view on the profound impact of glycosylation in maintaining the structural stability of SBA through unfolding dynamics. At higher temperature, the glycosylated SBA is relatively compact and

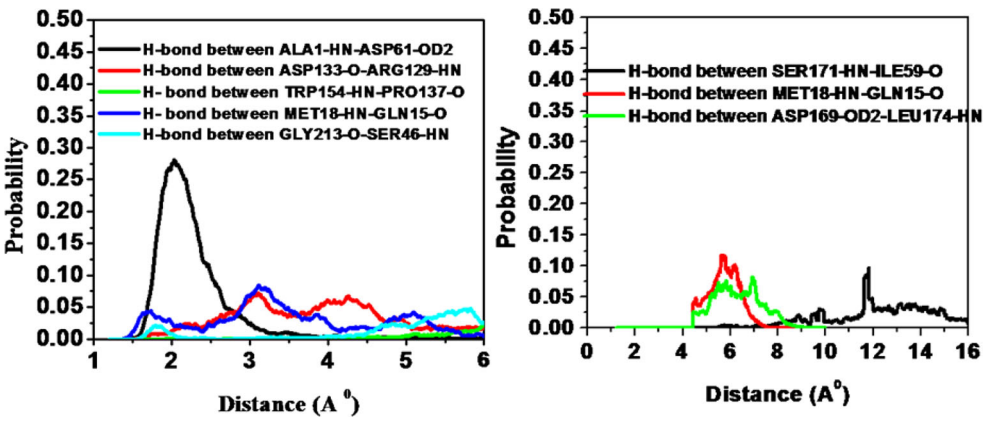

Fig. 8 Probability of forming H-bonds with distance in loop regions (**a**) glycosylated monomer at 380 K (**b**) nonglycosylated monomer at 380 K

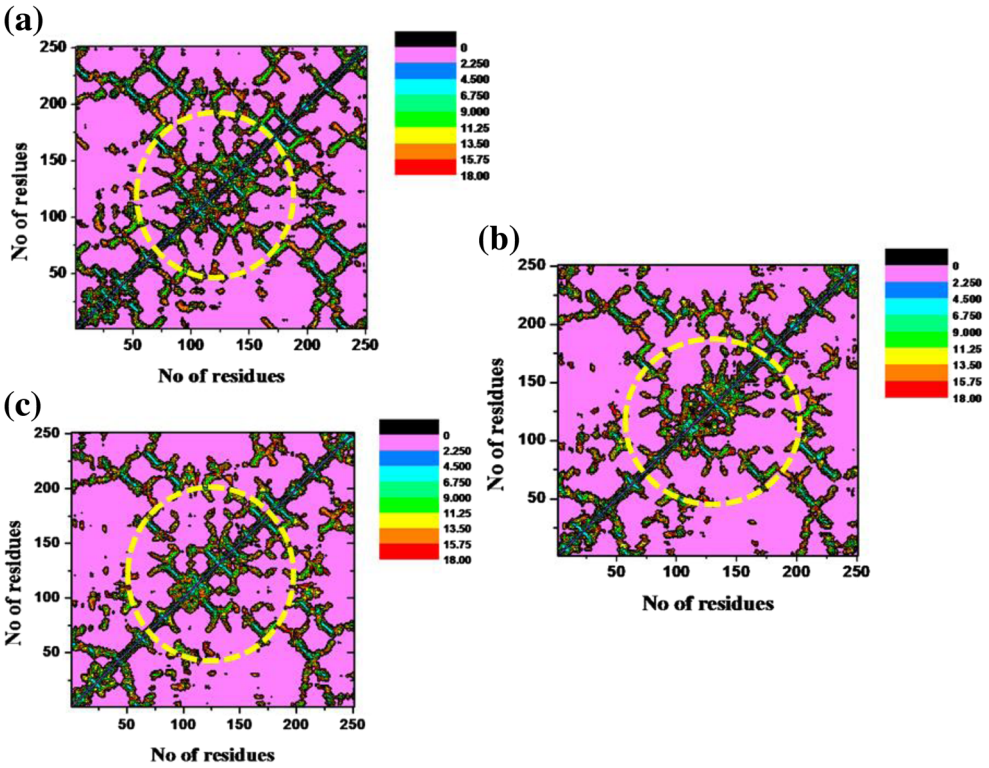

Fig. 9 Cα contact map (**a**) initial 10 ns time average structure of glycosylated SBA at 380 K (**b**) middle 10 ns time average structure of glycosylated SBA at 380 K (**c**) final 10 ns time average structure of glycosylated SBA at 380 K

stable, unlike NonGly_SBA. Also, the residues of Gly_SBA were less flexible than in its nonglycosylated form. These observations were further strengthened from the calculations of solvent accessible surface area. Further, the number of contacts and particularly hydrogen bonds, which are formed during the protein folding process and retain the stability of

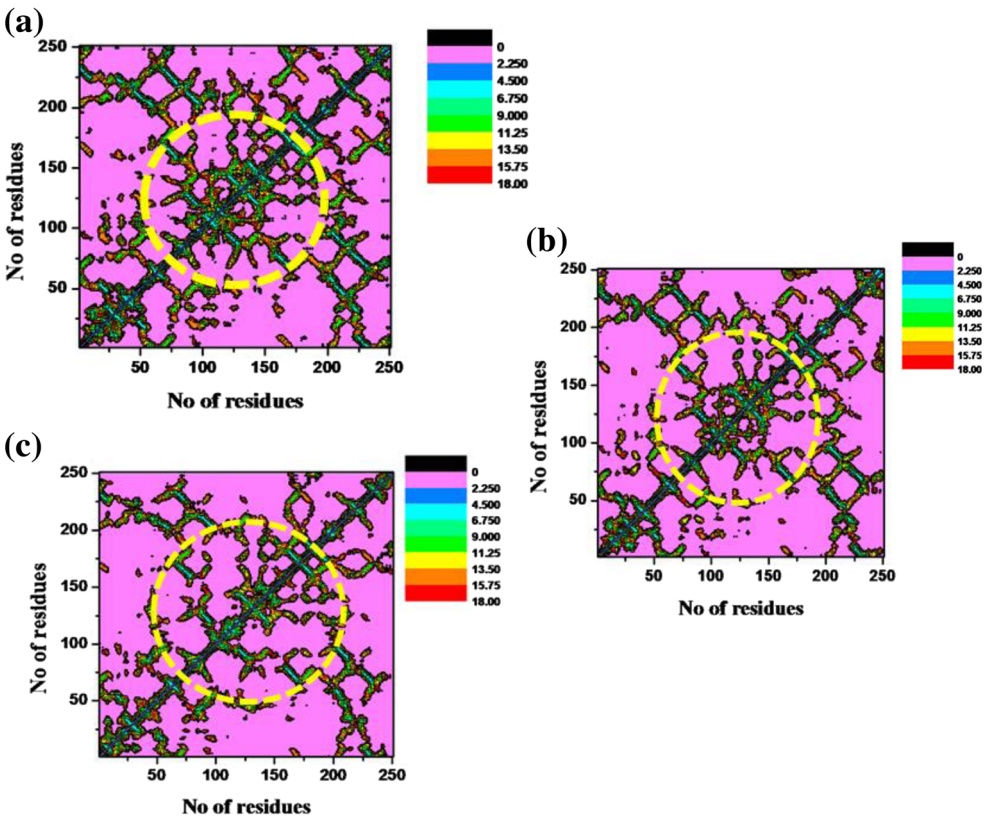

Fig. 10 Cα contact map (**a**) initial 10 ns time average structure of nonglycosylated SBA at 380 K (**b**) middle 10 ns time average structure of nonglycosylated SBA at 380 K (**c**) final 10 ns time average structure of nonglycosylated SBA at 380 K

Table 4 Some stable salt bridges present in the glycosylated monomer for the entire simulation time (values are given from averaging the data obtained from three individual simulations at initial 10 ns and final 10 ns)

Residues involved in the salt bridges	Initial salt bridge distance(Å)	Final salt bridge distance(Å)
ASP 23- LYS 44	2.55	3.83
ASP 215-ARG 85	3.29	3.38
GLU 39- LYS 36	2.55	3.98
ASP 192-LYS 150	3.70	2.70
ASP 118-LYS 100	3.42	3.24
ASP 195-LYS 197	2.49	2.77

secondary structures have significantly decreased in NonGly_SBA, have apparently slackened the protein. Hence, all these factors amalgamate to render the SBA unstable without the covalently attached glycan.

Conclusion

In this work, all atom molecular dynamics simulations were carried out for a well-studied lectin, soybean agglutinin with and without glycosylation at 298 K and 380 K, to understand in a more systematic way on how glycosylation affects the structure and dynamics. The overall global conformation of SBA was well conserved at normal temperature simulations as evidenced by the backbone RMSD of 2.5 Å relative to the crystal structure, while the protein size and compactness (solvent –accessible surface) generally varied weakly and unsystematically across simulations for glycosylated and nonglycosylated monomers, the high value of protein backbone-backbone hydrogen bond count was identified as a key, sensitive indicator of secondary-structure integrity of glycosylated monomer over that observed for its nonglycosylated counterpart under the thermal perturbations conditions investigated. Backbone bonds decreased significantly with temperature, reflecting entropy-enthalpy compensation. A number of salt bridges were identified, and the persistence of six of them ASP23-LYS44, ASP 215- ARG85, GLU39- LYS36, ASP192- LYS150, ASP118- LYS100, ASP195-LYS197 for glycosylated monomer across the temperatures 380 K, suggested their role in maintaining structural integrity of SBA, probably being strong and thus delay unfolding process. The terminal GlcNAc residues interact with the protein residues VAL161, PRO182 and SER225 *via* hydrophobic and *via* hydrogen bonding with ASN 9 and ASN 75. These hydrophobic interactions of carbohydrate-protein are crucial to maintain the folded structure of the protein. As expected, the strongest fluctuations were consistently found at solvent-exposed loops and turns. The most commonly observed loss of secondary structure (*i.e.,* backbone hydrogen bonds) occurred in exposed loops and ends of distinct β sheets.

Table 5 Some stable salt bridges present in the nonglycosylated monomer for the entire simulation time (values are given from averaging the data obtained from three individual simulations at initial 10 ns and final 10 ns)

Residues involved in the salt bridges	Initial salt bridge distance(Å)	Final salt bridge distance(Å)
GLU39- LYS 36	2.75	3.34
ASP 192-LYS 150	3.63	3.15
ASP 23 – LYS 44	2.81	2.68

Acknowledgments This work is supported by a project funded by the Department of Biotechnology, Government of India [No. BT/PR13421/BID/07/307/2009]. AS holds Bhatnagar Fellowship of the Council of Scientific and Industrial Research, India

References

1. Spiro, R.G.: Adv. Protein Chem. Glycoproteins. **27**, 349–467 (1973)
2. Lis, H., Sharon, N.: Protein glycosylation structural and functional aspects. Eur. J. Biochem. **218**(1), 1–27 (1993)
3. Varki, A.: Biological roles of oligosaccharides. All of the theories are correct. Glycobiology **3**(2), 97–130 (1993)
4. Dwek, R.A.: Toward understanding the function of sugars. Glycobiology **96**, 683–720 (1996)
5. Wang, C., Eufemi, M., Turano, C., Giartosio, A.: Soft materials: structure and dynamics. Biochemisty. **35**, 7299–7307 (1996)
6. Wormald, M.R., Dwek, R.A.: Glycoproteins: glycan presentation and protein-fold Stability. Structure **7**, 7155–7160 (1999)
7. Petrescu, A.J., Milac, A.L., Petrescu, S.M.: Statistical analysis of the protein environment of N-glycosylation sites: implications for occupancy, structure, and folding. Glycobiology **14**, 103–114 (2004)
8. Apweiler, R., Hermjakob, H., Sharon, N.: On the frequency of protein glycosylation, as Deduce from analysis of the SWISS-PROTdatabase. Biochim. Biophys. Acta **1473**, 4–8 (1999)
9. Yamaguchi, H.: Chaperone-like functions of N-glycans in the formation and stabilization of protein conformation. Trends Glycosci Glyc. **14**, 139–151 (2002)
10. Mitra, N., Sharon, N., Surolia, A.: Role of N-linked glycan in the unfolding pathway of Erythrina corallodendron lectin. Biochemistry **42**, 12208–12216 (2003)
11. Hanson, S.R.: The core trisaccharide of an N-linked glycoprotein intrinsically accelerates folding and enhances stability. Proc. Natl. Acad. Sci. U. S. A. **106**, 3131–3136 (2009)
12. Somnuke, P., Hauhart, R.E., Atkinson, J.P., Diamond, M.S., Avirutnan, P.: N- linked glycosylation of dengue virus NS1 protein modulates secretion, cell-surface expression, hexamer stability, and interactions with human complement. Virology **413**(2), 253–264 (2011)
13. O'Connor, S.E., Pohlmann, J., Imperiali, B.: Probing the effect of the outer saccharideresidue of *N*-Linked glycans on peptide conformation. J. Am. Chem. Soc. **123**, 6187–6188 (2001)
14. Bosques, C.J., Tschampel, S.M., Woods, R.J., Imperiali, B.: Effects of glycosylation on peptide conformation: a synergistic

experimental and computational study. J. Am. Chem. Soc. **126**, 8421–8425 (2004)
15. Shental-Bechor, D., Levy, Y.: Effect of glycosylation on protein folding: a close look at thermodynamic stabilization. Proc. Natl. Acad. Sci. U. S. A. **105**, 8256–8261 (2008)
16. Sola, R.J., Griebenow, K.: Effects of glycosylation on the stability of protein Pharmaceuticals. J. Pharm. Sci. **98**, 1223–1245 (2009)
17. Helenius, A., Aebi, M.: Intracellular functions of N-linked glycans. Science **291**, 2364–2369 (2001)
18. Li, S., Polonis, V., Isobe, H., Zaghouani, H., Guinea, R., Moran, T., Bona, C., Palese, P.: Chimeric influenza virus induces neutralizing antibodies and cytotoxic T cells against human immunodeficiency virus type 1. J. Virol. **67**, 6659–6666 (1993)
19. Yamaguchi, H., Uchida, M.: A chaperone-like function of intramolecular high- mannose chains in the oxidative refolding of bovine pancreatic RNase. B . J. Biochem. (Tokyo) **120**, 474–477 (1996)
20. Nishimura, I., Uchida, M., Inohana, Y., Setoh, K., Daba, K., Nishimura, S., Yamaguchi, H.: Oxidative refolding of bovine pancreatic RNases A and B promoted by Asn-Glycans. J. Biochem. (Tokyo) **123**, 516–520 (1998)
21. Dessen, A., Gupta, D., Sabesan, S., Brewer, C.F., Sacchettini, J.C.: X-ray crystal Structure of the soybean agglutinin cross-linked with a biantennary analog of the blood group I carbohydrate antigen. Bio-chemistry. **34**, 4933–4942 (1995)
22. Sinha, S., Gupta, G., Vijayan, M., Surolia, A.: Subunit assembly of plant lectins. Curr. Opin. Struct. Biol. **17**, 498–505 (2007)
23. Sinha, S., Mitra, N., Kumar, G., Bajaj, K., Surolia, A.: Unfolding studies on soybean agglutinin and concanavalin a tetramers: a comparative account. Biophys. J. **88**(2), 1300–1310 (2005)
24. Sinha, S., Surolia, A.: Oligomerization endows enormous stability to soybean agglutinin: a comparison of the stability of monomer and tetramer of soybean agglutinin. Biophys. J. **88**(6), 4243–4251 (2005)
25. Sinha, S., Surolia, A.: Attributes of glycosylation in the establishment of the unfolding pathway of soybean agglutinin. Biophys. J. **92**(1), 208–216 (2007)
26. Bernstein, F.C., Koetzle, T.F., Williams, G.J.: The Protein Data Bank: a computerbased archival file for macromolecular structures. J. Mol. Biol. **112**, 535–542 (1977)
27. Buts, L., Dao-Thi, M.H., Loris, R., Wyns, L., Etzler, M., Hamelryck, T.: Weak protein- protein interactions in lectins: the crystal structure of a vegetative lectin from the legume Dolichos biflorus. J. Mol. Biol. **309**(1), 193–201 (2001)
28. Bohne, A., Lang, E., Von der Lieth, C.W.: SWEET - WWW-based rapid 3D construction of oligo- and polysaccharides. Bioinformatics **15**, 767–768 (1999)
29. Brooks, B.R., Brooks 3rd, C.L., Mackerell Jr., A.D., Nilsson, L., Petrella, R.J., Roux, B., Won, Y., Archontis, G., Bartels, C., Boresch, S., Caflisch, A., Caves, L., Cui, Q., Dinner, A.R., Feig, M., Fischer, S., Gao, J., Hodoscek, M., Im, W., Kuczera, K., Lazaridis, T., Ma, J., Ovchinnikov, V., Paci, E., Pastor, R.W., Post, C.B., Pu, J.Z., Schaefer, M., Tidor, B., Venable, R.M., Woodcock, H.L., Wu, X., Yang, W., York, D.M., Karplus, M.: CHARMM: the biomolecular simulation program. Comput. Chem. **30**(10), 1545–1614 (2009)
30. Phillips, J.C., Braun, R., Wang, W., Gumbart, J., Tajkhorshid, E., Villa, E., Chipo, C., Skeel, R.D., Kalé, L., Schulten, K.J.: Scalable molecular dynamics with NAMD. Comput. Chem. **26**, 1781–1802 (2005)
31. Jorgensen, W.L., Chandrasekhar, J., Madura, J.D., Impey, R.W., Klein, M.L.: Comparison of simple potential functions for simulating liquid water. J. Chem. Phys. **79**, 926–935 (1983)
32. Martyna, G.J., Tobias, D.J., Klein, M.L.: Conformational study of N-terminal prion peptides by molecular dynamics simulations. J. Chem. Phys. **101**, 4177–4189 (1994)
33. Darden, T., York, D., Pedersen, L.G.: Particle mesh Ewald: an Nlog(N) method for Ewald sums in large systems. Chem. Phys. **98**, 10089–10092 (1983)
34. Ryckaert, J.P., Ciccotti, G., Berendsen, H.J.C.: Numerical integration of the Cartesian equations of motion of a system with constraints: molecular dynamics of n-alkanes. J. Comput. Phys. **23**, 327–341 (1977)
35. Humphrey, W., Dalke, A., Schulten, K.: VMD - visual molecular dynamics. J. Mol. Graph. **14**, 33–38 (1996)
36. Homans, S.W., Dwek, R.A., Rademacher, T.: Tertiary structure in N-linked oligosaccharides. Biochemistry **26**, 6553–6560 (1987)
37. Homans, S.W., Pastore, A., Dwek, R.A., Rademacher, T.W.: Structure and dynamics in oligomannose-type oligosaccharides. Biochemistry **26**, 6649–6655 (1987)
38. Qasba, P.K., Balaji, P.V., Rao, V.S.R.: Molecular dynamics simulations of oligosaccharides and their conformation in the crystal structure of lectin-carbohydrate complex: importance of the torsion angle ψ for the orientation of α1,6-arm. Glycobiology **4**, 805–815 (1994)
39. Petrescu, A.J., Petrescu, S.M., Dwek, R.A., Wormland, M.R.: Statistical analysis of the protein environment of *N*-glycosylation sites: implications for occupancy, structure, and folding. Glycobiology **14**(2), 103–114 (2003)
40. Dorland, L., van Halbeek, H., Vleigenthart, J.F., Lis, H., Sharon, N.: Primary structure of the carbohydrate chain of soybean agglutinin. A reinvestigation by high resolution 1H NMR spectroscopy. J. Biol. Chem **256**, 7708–7711 (1981)
41. Olsen, L.R., Dessen, A., Gupta, D., Sabesan, S., Sacchettini, J.C., Brewer, C.F.: X-ray crystallographic studies of unique cross-linked lattices between four isomeric biantennary oligosaccharides and soybean agglutinin. Biochemistry **36**, 15073–15080 (1997)
42. Kaushik, S., Mohanty, D., Surolia, A.: ROLE of glycosylation in structure and stability of *Erythrina corallodendron* lectin (EcorL): a molecular dynamics study. Protein Sci. **20**, 465–481 (2010)
43. Mitra, N., Sinha, S., Ramya, T.N.C., Surolia, A.: N-linked oligosaccharides as out-fitters for glycoprotein folding, form and function. Trends in Biochem. Sci. **31**, 156–163 (2006)
44. Kaushik, S., Mohanty, D., Surolia, A.: Molecular dynamics simulations on *ParIntercerebralis Major* Peptide-C (PMP-C) reveal the role of glycosylation and disulfide bond Structura stability and function. J. Bimolecular Struct. Dyn. J. Bimolecular Struct Dyn. **29**, 905–921 (2012)
45. Gruia, A.D., Fischer, S., Smith, J.C.: Molecular dynamics simulation reveals a Surface salt bridge forming a kinetic trap in unfolding of truncated Staphylococcal Nuclease. Proteins **50**, 507–515 (2003)
46. Chan, C.H., Yu, T.H., Wong, K.B.: Stabilizing salt-bridge enhances protein thermostability by reducing the heat capacity change of unfolding. PLoS One **6**(6), e21624 (2011)